# Renormalization for Collective Motion within a Truncated Space of the Spherical Shell Model. II. Projected Frame in a Schematic Model

M. HARVEY AND H. C. LEE

Atomic Energy of Canada Limited, Chalk River Nuclear Laboratories, Chalk River, Ontario, Canada KOJ 1JO

AND

#### Р. Амют

Université Laval, Cité Universitaire, Québec 10, Québec, Canada G1K 7P4

Received April 12, 1977

In paper I, [Ann. Phys. (N.Y.) 94 (1975)] the matrix elements of effective operators in an intrinsic frame of the spherical shell model, that were determined by an iterative, renormalization technique, were shown to be analytically equivalent to those from a deformed, unrestricted Hartree-Fock model for the case of <sup>20</sup>Ne with a schematic quadrupole-quadrupole Hamiltonian. This paper shows the numerical comparison of the results from the renormalized spherical shell model and the projected, deformed Hartree-Fock model in the laboratory frame with states of definite angular momentum. Good agreement is found for the full iterative, renormalization results and those from the variation-after-projection Hartree-Fock model.

#### 1. Introduction

The standard spherical shell model calculations (SSSM) involve the description of nuclear states in terms of configurations having a spherical core, from the filling of the lowest single particle orbitals, with the remaining particles distributed among a few valence orbitals (cf. [1]). The use of effective charges in the calculations for quadrupole moments and transitions is but one indication, however, that the nucleus has structure beyond that described by the model wavefunctions. If the object of a shell-model calculation is to learn something about the structure of the nucleus, then it is clearly as important to study the hidden structure buried in the effective charge phenomena as it is to study the structure of the model wavefunctions themselves.

The attempts that have been made to supplement the model wavefunctions by a systematic addition of low-order perturbation terms have not been completely successful in explaining the origin of the effective charges and have never considered

examples with more than two valence particles (cf. [2]). Such is the plethora of higherorder perturbation terms that a study of contributions order-by-order would seem doomed to failure.

In this series of papers our approach has been different. We attempt to recognize a priori the physical structures that, for some nuclei, are believed to be missing from the model wavefunctions, and then identify the types of perturbation terms that describe these features. Necessarily we must be prepared to accept some types of perturbation terms of very high order if these are seen to be important from the physical point of view, just as we shall feel free initially to ignore some types of low-order terms which do not seem to play a role in the phenomena under study. Throughout our approach we always insist on a consistent renormalization: thus, whatever perturbation terms are introduced into the calculation of effective operators, similar terms must also be introduced into the calculation for effective interactions to deduce the corresponding effects on the energy spectrum.

The big question of course is what physical properties are believed to be missing from the standard spherical shell model wavefunctions. Here we turn to other models for guidance. For some light nuclei, like <sup>20</sup>Ne, the unrestricted deformed Hartree–Fock model has been remarkably successful in explaining the magnitudes of quadrupole matrix without the use of effective charges and also a reasonably correct level density within a band using the bare reaction matrix (cf. [3]). The success of this model seems to hinge on the self-consistent generation of the deformed intrinsic state. Since <sup>20</sup>Ne is also a typical spherical shell model nucleus, it is certainly relevant to ask what series of perturbation terms must one consider within the framework of the renormalized spherical shell model that will recapture the self-consistency of the deformed Hartree–Fock model.

In an earlier paper ([4], hereafter referred to as I) we considered the deformation in the intrinsic state for <sup>20</sup>Ne for a simple schematic Hamiltonian of the form

$$H_A = h_0 + v_Q \tag{1.1}$$

with

$$v_Q = \hbar \omega_0 x \sum_{i < j} Q(i) \cdot Q(j)[X_{ij}], \qquad (1.2a)$$

$$Q_q(i) = \left(\frac{16\pi}{5}\right)^{1/2} \frac{r_i^2}{b_0^2} Y_q^2(\theta_i \phi_i), \tag{1.2b}$$

$$[X_{ij}] = a_0 + a_{\sigma}(\sigma_i \cdot \sigma_j) + a_{\tau}(\tau_i \cdot \tau_j) + a_{\sigma\tau}(\sigma_i \cdot \sigma_j)(\tau_i \cdot \tau_j)$$
 (1.3)

and

 $h_0$  is a spherical harmonic oscillator  $(\hbar\omega_0 \equiv \hbar^2/mb_0^2)$ .

The exchange mixture of  $v_0$  was so chosen that

$$A^{11} + 9A^{33} = 3(A^{13} + A^{31}) = 8 (1.4)$$

with

$$A^{2T+1,2S+1} = \langle TS \mid [X] \mid TS \rangle$$

where  $|TS\rangle$  is a two-body state with isospin T and spin S. With this particular exchange mixture, the Hartree-Fock Hamiltonian for an N=Z nucleus has precisely the structure of a deformed oscillator

$$h_{\rm HF} \equiv h_0 - \hbar \omega_0 [\delta Q_0 + \gamma (Q_2 + Q_{-2})]$$
 (1.5)

where

$$-\delta = x \langle Q_0 \rangle_{\delta} \tag{1.6a}$$

and

$$\gamma = x \langle Q_2 + Q_{-2} \rangle_{\delta}. \tag{1.6b}$$

The expectation values in Eq. (1.6) are taken with respect to the lowest many particle, deformed eigensolution  $\chi_{\delta}$  of  $h_{\delta}$ .

The study in I was restricted to the structure of the intrinsic state  $\chi_{\delta}$  relative to that part of it  $(\chi_0)$  that lies in the standard spherical shell model space of closed 1s and 1p shells and four particles in the (2s, 1d) shell. The state  $\chi_0$  is in fact the intrinsic state of the leading representation in the (spherical)  $SU_3$  model [5]. It was shown in I (Eq. (4.7)) how, for an axially symmetric system like <sup>20</sup>Ne, the self-consistent condition in Eq. (1.6a) could be recast into an equation representing the perturbation expansion of  $\langle Q_0 \rangle_{\delta}$  with respect to the state  $\chi_0$ . Thus the same equation can be interpreted either as the self-consistent condition for the deformed Hartree–Fock model or as the perturbative equation for the renormalization of the quadrupole operator in the spherical shell model. It was a relatively simple exercise therefore to examine the equation term-by-term to identify the types of perturbation terms that are equivalent to self-consistent deformation. Of course, since the Hartree–Fock state itself is an approximation to the lowest eigensolution of  $H_A$ , not every perturbation term need appear in this "collective renormalization" of the quadrupole operator. This selection, however, is consistent with the spirit of our approach.

An interesting principle of "consistent renormalization" was noted in I which, for the schematic Hamiltonian of Eq. (1.1), allows certain classes of higher-order terms to be easily generated from a few low-order terms. This is achieved by replacing all quadrupole matrix elements within the valence space, as they appear within a perturbation term, by their renormalized values. Since the renormalized value is not known until the perturbation terms for the renormalized quadrupole operator have been summed, it is clear that, in general, the solution can only be found iteratively. This iterative solution is precisely equivalent to the self-consistency involved in the generation of the deformation in the Hartree–Fock method. In I we introduced a "black-dot" vertex renormalization to perturbation diagrams indicating that the renormalized quadrupole matrix elements should be used. If only the first-order

bubble perturbation terms are considered, then the black-dot vertex renormalization is equivalent to building up the open-shell RPA series. As noted in I, however, it is necessary to include also the black-box vertex renormalization of Barrett and Kirson ([2] with particle-particle as well as particle-hole interactions) if agreement with deformed Hartree-Fock is to be reached. The black-dot vertex renormalization, together with the black-box, generate very exotic perturbation terms (cf. Fig. 11 in I).

In this paper we extend the results of I into the laboratory frame. Now the "model" states for <sup>20</sup>Ne are the band of states having good angular momentum J=0,2,4,6, and 8 belonging to the leading ( $\lambda\mu=80$ ) representation of  $SU_3$ . Using the series of perturbation terms for "collective renormalization" we deduce the enhancements for quadrupole matrix elements within the band and the renormalized energy spectrum. Results of the calculation agree well with those from a variation-after-projection, unrestricted, deformed Hartree-Fock calculation (VPHF).

The results of the VPHF calculation are presented in Section 2 prior to the discussions in Section 3 on the results of the renormalization in the spherical shell mode. In the summary of Section 4 we briefly hint at how the procedures of these two papers are being generalized for a realistic Hamiltonian.

We finish this introduction with a word of clarification with regard to the unusual exchange mixture in Eq. (1.4). Most quadrupole-quadrupole interactions in the literature have been used with a Wigner exchange mixture ( $a_{\sigma} = a_{\tau} = a_{\sigma\tau} \equiv 0$ ) but exchange contributions in two-body matrix elements are ignored: thus Mottelson [6] has shown that the Hartree (no exchange) field of  $H_A$  in Eq. (1.1) with Wigner exchange has the structure of the deformed oscillator. Unfortunately it is not obvious which exchange terms in the renormalized spherical shell model must correspondingly be ignored to achieve the same result. For clarity therefore we have resorted to the exchange mixture in Eq. (1.4) with which the exchange terms in the Hartree-Fock field exactly cancel, thus leading once again to Mottelson's result. Now, however, we consider all exchange terms in the two-body matrix elements of the renormalization perturbation series with the satisfaction that we have performed a consistent calculation.

# 2. THE UNRESTRICTED, PROJECTED HARTREE-FOCK APPROACH

In the projected Hartree-Fock (PHF) method [3, 7] the energies  $E_J$  of the lowest eigenstates of  $H_A$  are approximated by the expectation value of the Hamiltonian with respect to a state  $\psi_J$  of angular momentum J projected from the Hartree-Fock state  $\chi_\delta$  where  $\chi_\delta$  is the lowest many particle solution of the Hartree-Fock Hamiltonian  $h_{\rm HF}$ . Thus

$$h_{\mathsf{H}-\mathsf{F}}\gamma_{\delta} = \mathscr{E}\gamma_{\delta}, \tag{2.1a}$$

$$\psi_I = P^I \chi_\delta \,, \tag{2.1b}$$

$$E_I = (\psi_I \mid H_A \mid \psi_I). \tag{2.1c}$$

Experience has shown [3] that a better estimate for the structure of each state (especially for high J) is given by allowing the intrinsic state to vary in some collective way for each J. In practise this is achieved by imposing some single particle (collective) constraint  $\lambda Q$  on the Hartree-Fock field, determining the solution  $\chi_{\theta}(\lambda)$  in terms of the strength  $\lambda$  of the constraint, and then minimizing the energy  $E_J(\lambda)$  with respect to  $\lambda$  for each J. The energies derived in this way yield the variation after projection Hartree-Fock approximation (VPHF).

For the schematic Hamiltonian  $H_A$  applied to <sup>20</sup>Ne we follow Cusson and Lee [3] by taking the constraint to be the q=0 component of the quadrupole operator in Eq. (1.2b). Thus

$$h_{\rm H-F}(\lambda) = h_{\delta} + \lambda \hbar \omega_0 Q_0 \equiv h_{\delta'}$$
.

Since the Hartree-Fock field for  $H_A$  has the structure of a deformed oscillator  $(h_{\delta})$ , that for the constrained system also has the deformed oscillator structure but with a different deformation

$$\delta' = -x \langle Q_0 \rangle_{\delta'} + \lambda.$$

Thus, for the Hamiltonian  $H_A$ , the VPHF soluiton with  $Q_0$  constraint is equivalent to projecting J from the lowest many particle state of a deformed oscillator and then varying the deformation of the oscillator to achieve a minimum for each J.

The PHF and VPHF calculations for <sup>20</sup>Ne with the Hamiltonian  $H_{\lambda}$  were done using the computer code EVALIN written by Cusson and Lee [3]. Here the single particle deformed oscillator states are approximated by an expansion over five major shells of the orbits of the spherical oscillator  $h_0$ . Results of the variation calculation are shown in Fig. 1 for a  $v_0$  strength x = -0.003. Plotted on the abscissa is the strength  $\lambda$  of the  $Q_0$ -constraint and, equivalently, the  $\beta$ -deformation of the constrained intrinsic state. The energy is given in units of  $\hbar\omega_0$  ( $\approx 15$  MeV for <sup>20</sup>Ne) relative to the expectation value of  $h_0$  in the spherical shell model ( $\langle h_0 \rangle_0 = 50 \ \hbar\omega_0$ ).

It is interesting to note the similarity of Fig. 1 with Fig. 3 of the paper by Cusson and Lee [3] even though they used the "realistic" interaction of Saunier and Pearson [8] in their constrained Hartree-Fock calculation. We see clearly, for example, the antistretching feature whereby states of higher angular momentum prefer smaller intrinsic deformations. Such a comparison gives confidence that the gross features determining collective motion in the realistic calculation also exist in our simpler schematic model and that later features of the renormalization calculation are also meaningful.

For our schematic model, when the strength of the constraint  $\lambda \approx -0.05$  the deformation arising from  $v_Q$  is canceled, i.e., the single particle field is that of the spherical oscillator  $h_0$ . The spectrum at this point is shown on the extreme left-hand side of the curves in Fig. 1 and represents the spectrum in the (bare) spherical shell model with states arising from the projection of J from a many particle intrinsic state of the spherical oscillator in a Cartesian representation having the same quantum

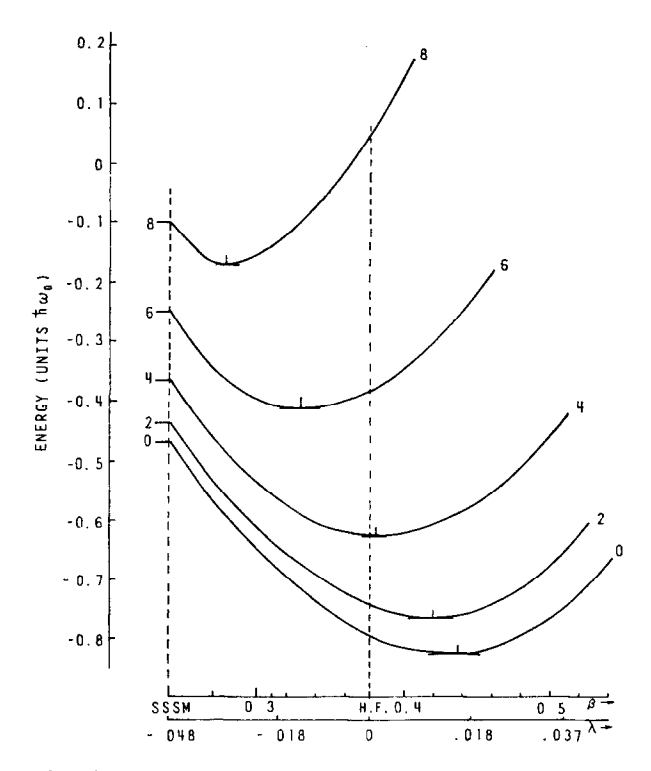


Fig. 1. Energy of projected states of given J for the schematic Hamiltonian of Eq. (1.1) relative to the expectation value of  $h_0$  in the spherical shell model configuration:  $\langle h_0 \rangle_0 = 50 \, \hbar \omega_0$ . On the abscissa is shown the  $\beta$ -deformation of the constrained intrinsic state with the constraining parameter  $\lambda$ . The points of each curve on the vertical dashed line mark the spectra for the SSSM and PHF approximation as marked. The VPHF spectrum is given by the minima for each curve.

distribution  $S_k = \sum_i (n_k(i) + \frac{1}{2})$ , k = 1, 2, 3, as the fully deformed intrinsic Hartree-Fock state:  $n_k(i)$  is the number of quanta in the kth-direction on the ith particle. The spherical shell model states generated in this way [5] are those belonging to the leading  $(\lambda \mu) = (80)$  representation of the group  $SU_3$ . Thus already we see in Fig. 1 that the effect of deformation is greater for the states for smaller angular momentum. We must expect therefore that the renormalization of operators within the spherical shell model that takes this deformation into account should be greater for the low energy states.

# 3. THE RENORMALIZED SPHERICAL SHELL MODEL APPROACH

# Bare Approximation

We choose as model Hamiltonian the spherical oscillator  $h_0$ , and hence the residual interaction for the schematic Hamiltonian of Eq. (1.1) is identical to the quadrupole—

quadrupole potential  $v_Q$  of Eq. (1.2a). The model space for <sup>20</sup>Ne is chosen to consist of configurations having closed 1s and 1p shells with two neutrons and two protons in the (2s, 1d) shell. The potential  $v_Q$  acting within the model space is very similar to the quadrupole-quadrupole potential of the  $SU_3$  model and so we have approximated the bare calculation by considering just the states of the leading  $(\lambda \mu) = (80)$  representation of  $SU_3$ . These states have maximum orbital symmetry [44444] and hence total intrinsic spin and isotopic spin S = T = 0. The (80) representation contains states corresponding to the ground state band of <sup>20</sup>Ne having J = 0, 2, 4, 6, and 8.

The "bare" energy of states within the (80)-representation is found, by the method of Elliott and Harvey [9], to have the form

$$((80)J \mid v_O \mid (80)J) = x\hbar\omega_0[1088 - 12J(J+1)]/7. \tag{3.1}$$

The bare spectrum is shown in Fig. 2 (spectrum a) in units of  $\hbar\omega_0$  for x=-0.003 and is identical to the spectrum at the LHS of Fig. 1. Clearly a comparison between

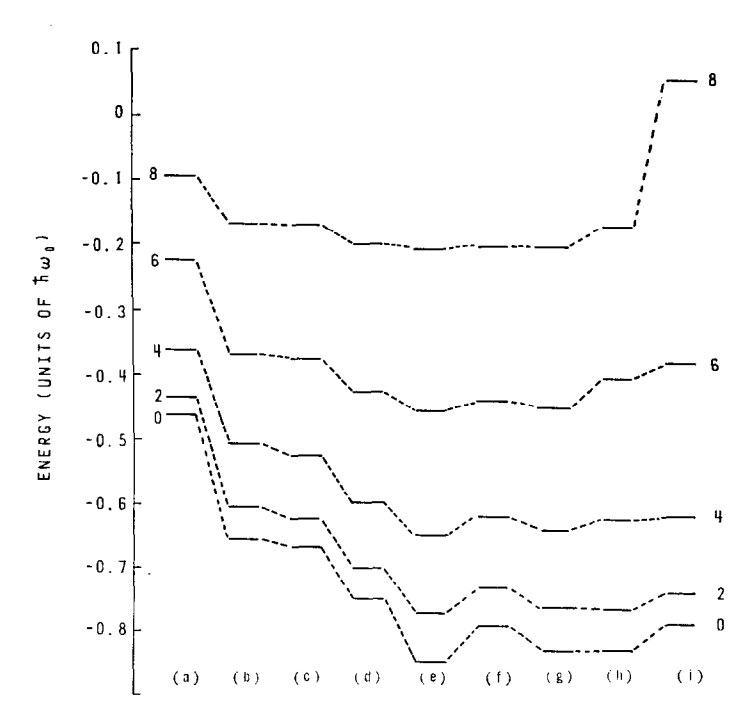


Fig. 2. Energy spectra for the schematic Hamiltonian of Eq. (1.1) (relative to  $\langle h_0 \rangle_0$ ) under various approximations (a) bare (SSSM); (b) bubble (first order); (c) bubble + black-box vertex renormalization; (d) black-dot renormalization of the bubble approximation; (e) black-box and black-dot; (f) black-box, black-dot, and intermediate bubble generation with the black-box taken only to second order; (g) as in (f) but for all orders of the black-box vertex renormalization; (h) the variation-after-projection Hartree-Fock approximation; (i) the projected Hartree-Fock approximation.

the bare spectrum and the VPHF spectrum (Fig. 2h) shows that renormalization due to deformation effects are considerable.

All isoscalar quadrupole reduced matrix elements will be compared to those arising in the (80)-representation to define state-dependent enhancement factors  $\epsilon_{IJ'}$ ; i.e.,

$$(J \parallel Q \parallel J') \equiv \epsilon_{JJ'}((80)J \parallel Q \parallel (80)J'). \tag{3.2}$$

Reduced matrix elements are defined in the Wigner-Eckart theorem

$$(JM \mid Q_{\sigma} \mid J'M') = (J'2M'q \mid JM)(J \parallel Q \parallel J')/(2J+1)^{1/2}.$$

Thus enhancement factors for the quadrupole matrix elements in the bare approximation are all unity by definition. Those for the matrix elements in the VPHF approximation (x = -0.003) shown in Fig. 3 (open circles joined by dashed lines) range from 1.2 to 1.8.

Comparison of experimental data on B(E2)-transitions in <sup>20</sup>Ne with the bare model having  $\hbar\omega_0 = 41A^{-1/3}$  reveals the need for phenomenological isoscalar quadrupole enhancement factors with  $\epsilon \sim 2$ . We could have forced our model to yield such large factors by increasing |x| but this would bring the calculation close to the unphysical

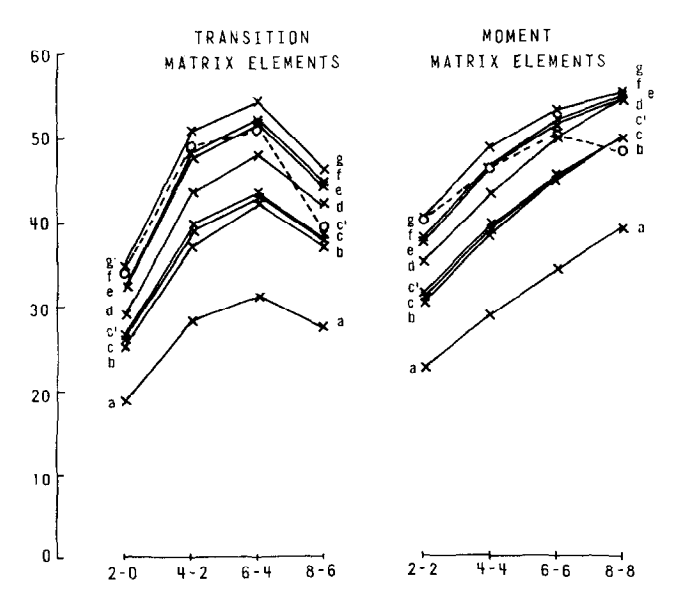


Fig. 3. The magnitude of the reduced quadrupole matrix elements  $(J \mid Q \mid J')$  (dimensionless units) in the various approximations (a)–(g) listed in Fig. 2. The points labeled (c') refer to the blackbox, bubble, intermediate-bubble-generation approximation for which the energy spectrum is exactly the same as (c). Note that all the transition matrix elements are positive while those for the moments are negative. The results for the VPHF approximation are shown by the open circles connected by the dashed lines.

deformation instability that the schematic Hamiltonian possesses as was discussed in I. Since our main aim was to study the technique for collective renormalization itself, we have chosen the smaller value |x| = 0.003 (and hence  $\epsilon_{JJ'} < 2$ ) to avoid too many spurious effects.

# **Bubble Approximation**

The "excluded" spherical shell model configurations are restricted to those differing from the "model" states of the (80)-representation by a particle lifted across two major oscillator shells. The three different types of excluded states will be given the label N which describes the  $[1s \rightarrow (2s, 1d)]$  excitation for N = 1;  $[1p \rightarrow (2p, 1f)]$  for N = 2; and  $[(2s, 1d) \rightarrow (3s, 2d, 1g)]$  for N = 3. The off-diagonal matrix elements of the residual interaction  $v_0$  coupling these excluded configurations to the (80)-states are expressible in terms of products of a reduced quadrupole matrix element within the (80)-representation and the single-particle, reduced quadrupole matrix element associated with the  $[h \to p]$  excitation (see the later Eq. (3.7)). The part of the quadrupole operator that excites a particle across two major shells transforms according to the (20) representations of  $SU_3$ : the part that acts within a major shell transforms according to the (11) representation but, since this part is identical to a generating operator of  $SU_3$ , it effectively acts like a scalar as far as selection rules are concerned. Consequently the residual interaction can be considered to effectively transform according to the (20) representation of  $SU_3$  as far as the coupling between the model and excluded space is concerned. Thus the only  $[h \rightarrow p]$  "excluded" states that need be considered are those classified according to the  $SU_3$  representations

$$(\lambda \mu) = (80) \times (20) = (10, 0) + (81) + (62).$$

Since the  $v_Q$  interaction is a central force we select also just the states of maximum orbital symmetry. Thus the only excluded configurations considered in our renormalization have the totally antisymmetric structure

$$|N = 1, (\lambda \mu) KJ\rangle \equiv |1s^3 1p^{12}(2s, 1d)^5_{(\lambda \mu)KJ}\rangle,$$
 (3.3a)

$$|N = 2, (\lambda \mu) KJ\rangle \equiv |1s^{4}\{\{1p^{11}(2p, 1f)^{1}\}_{(20)} (2s, 1d)^{4}_{(80)}\}_{(\lambda \mu) KJ}\rangle,$$
 (3.3b)

$$|N = 3, (\lambda \mu) KJ\rangle = |1s^4 1p^{12} \{(2s, 1d)_{(60)}^3 (3s, 2d, 1g)_{(40)}^1\}_{(\lambda \mu) KJ},$$
 (3.3c)

with  $(\lambda \mu) = (10, 0)$ , (81), or (62) and maximum orbital symmetry is to be understood, i.e., S = T = 0. We note that antisymmetry precludes a  $(\lambda \mu) = (10, 0)$  representation in the case N = 1.

The nonzero matrix elements of the first-order approximation to the wave operator can thus be written

$$\langle N(\lambda \mu) KJ \mid \vec{W}^{(1)} \mid (80) 0J \rangle = (N(\lambda \mu) KJ \mid v_Q \mid 80 0J)/(-2\hbar\omega_0).$$
 (3.4)

The matrix elements of  $v_Q$  have been deduced using the method of Elliott and

Harvey [9]. Using the standard equations for renormalization of a single body operator (cf. [4] and [10]) one can now deduce the first-order correction  $\epsilon_{JJ}^{(1)}$  to the quadrupole matrix elements acting within the (80)-model space

$$\epsilon_{JJ}^{(1)}((80) \ 0J \parallel Q \parallel (80) \ 0\bar{J}) = ((80) \ 0J \parallel Q \parallel (80) \ 0\bar{J}) 
+ \sum_{N\lambda\mu K} [(80 \ 0J \mid \widetilde{W}^{(1)} \mid N(\lambda\mu) \ KJ)(N\lambda\mu KJ \parallel Q \parallel (80) \ 0\bar{J}) 
+ (80J \parallel Q \parallel N\lambda\mu K\bar{J})(N\lambda\mu K\bar{J} \mid \widetilde{W}^{(1)} \mid 80 \ 0\bar{J})].$$
(3.5)

The two last correction terms on the RHS we represent diagrammatically by Fig. 4

Fig. 4. Schematic representation of the first order renormalization terms of a one-body operator.

and refer to them loosely as the "bubble" correction. The enhanced reduced matrix elements  $\epsilon_{IJ}((80)\ 0J\parallel\ \parallel (80)\ 0\bar{J})$  are reproduced in Fig. 3 (crosses labeled b) for x=-0.003.

The energy spectrum is evaluated from the expression

$$\langle (80) \ 0J \ | \ \nu^{(1)} \ | \ (80) \ 0J \rangle = ((80) \ 0J \ | \ v_O \ | \ (80) \ 0J)$$

$$+ \sum_{N\lambda\mu K} (80 \ 0J \ | \ v_O \ | \ N\lambda\mu KJ)(N\lambda\mu KJ \ | \ \vec{W}^{(1)} \ | \ 80 \ 0J) \quad (3.6)$$

and is shown in column b of Fig. 2.

#### Black-Dot Renormalization

We write the off-diagonal matrix element of  $v_Q$  as it appears in Eq. (3.4) in the form

$$\langle N\lambda\mu KJ \mid v_Q \mid 80 \ 0J \rangle$$
  
=  $\alpha_{N\lambda\mu K} \sum_{J'} ((20) \ 2(80) \ J' \mid (\lambda\mu) \ KJ) \ W(JJ' \ 02; \ 2J) \ q_N \langle 80J' \parallel Q \parallel 80J \rangle$  (3.7)

where  $q_N$  represents particle-hole reduced quadrupole matrix elements of Q across two major shells, thus

$$q_{(N=1)} = \langle \{1s^{-1}(2s, 1d)\}_{(20)2} || Q || 0 \rangle,$$
  

$$q_{(N=2)} = \langle \{1p^{-1}(2p, 1f)\}_{(20)2} || Q || 0 \rangle,$$
  

$$q_{(N=3)} = \langle \{2s, 1d\}^{-1}(3s, 2d, 1g)\}_{(20)2} || Q || 0 \rangle.$$

The factor ((20) 2 (80)  $J' \mid (\lambda \mu) KJ$ ) represents an  $SU_3$  Clebsch-Gordan coefficient [11, 12] with K a convenient orthonormal labeling of states with the same J within a representation; W(abcd:ef) is an  $SU_2$  Racah coefficient [13]. The factor  $\alpha_{N\lambda\mu K}$  in Eq. (3.7) absorbs all the spectroscopic factors representing the antisymmetry of states, and strength and exchange of  $v_Q$ . In practice we have evaluated the LHS of Eq. (3.7) using the method of Elliott and Harvey [9] and then deduced the  $\alpha_{N\lambda\mu K}$  factors.

The off-diagonal matrix elements of  $v_O$  in the form of Eq. (3.7) display, through Eq. (3.4), the dependence of the wave operator  $\vec{W}^{(1)}$  on the quadrupole matrix elements that transform within the (80)-model space. According to the principle of consistent renormalization these matrix elements in  $\vec{W}^{(1)}$  should be replaced by the renormalized values; i.e.,

$$\langle (80) \ 0J' \parallel Q \parallel (80) \ 0J \rangle \to \epsilon_{J'J} \langle 80 \ 0J' \parallel Q \parallel (80) \ 0J \rangle.$$
 (3.8)

With the matrix elements of  $\overline{W}^{(1)}$  having such a dependence on  $\epsilon_{J'J}$  we see that Eq. (3.5) can be solved iteratively for the various factors  $\epsilon_{J'J}$ . Such an iterative solution based on the first-order wave operator we represent schematically by the diagram in Fig. 5 and call this the black-dot (bd) approximation. The steps in the

Fig. 5. Schematic representation of the black-dot approximation to the renormalization of the quadrupole operator.

iterative solution are shown by the crosses on the lines labeled d in the diagrams of Fig. 6 which shows the enhancement value  $\epsilon_{J'J}$  after the *n*th iteration on the ordinate plotted against the  $\epsilon_{J'J}$  at the n-1 iteration on the abscissa. (In zeroth order all  $\epsilon_{J'J} \equiv 1$ .) Clearly self-consistency is reached at the 45° line. The solutions after five iterations have been plotted in Fig. 3 (crosses labeled d). Having found the self-consistent value for  $\epsilon_{J'J}$  in this approximation the compatible energy spectrum is deduced from Eq. (3.6) using Eq. (3.8) in the definitions for the matrix elements of  $W^{(1)}$  (Eq. (3.4)). The spectrum in this bd-approximation is shown in Fig. 2, spectrum d. We note that the energy difference for the  $J=0^+$  ground state between the bubble approximation (spectrum b) and the VPHF (spectrum h) is about halved by the black-dotting procedure which agrees qualitatively with the corresponding changes in the calculation for the intrinsic energies in 1 (see I, Table I).

# Black-Box Vertex Renormalization

In I it was shown that the black-box (bb) vertex renormalization with intermediate states restricted to  $2\hbar\omega$ -excitation was significant as far as reproducing the results of

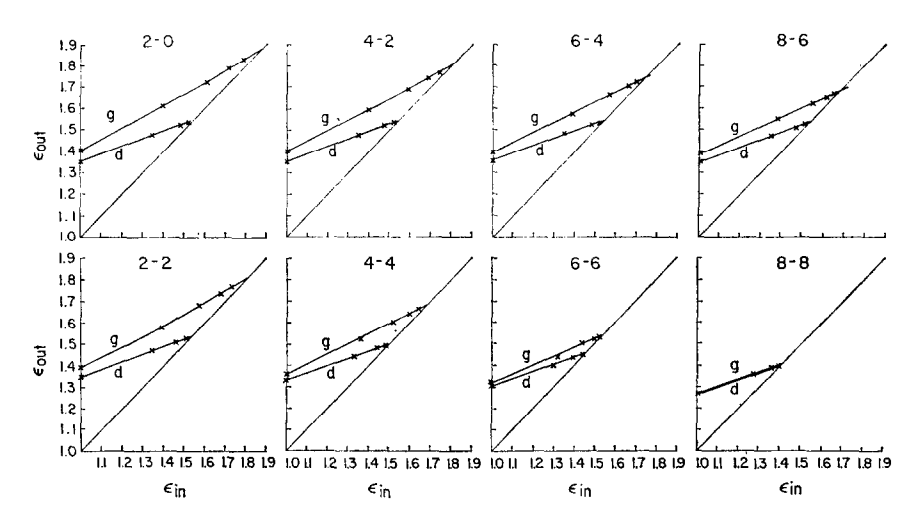


Fig. 6. Iterative sequences for the enhancement factors  $\epsilon_{JJ'}$  in the bb-bd-IBG (g) approximation and in the simple bd (d) approximation. Each diagram (J-J') corresponds to a particular  $(J \parallel Q \parallel J')$  matrix element. Plotted on the abscissa is the enhancement factor  $\epsilon_{JJ'}$  put into the iterative equation and on the ordinate the  $\epsilon_{JJ'}$  factor calculated from the iterative equation. The crosses correspond to the iterative sequence beginning at  $\epsilon_{JJ'}(in) \equiv 1$ .

the deformed self-consistent calculation with the schematic Hamiltonian. In order to put such a feature into the present calculation in the laboratory frame it is necessary to compute the matrix elements of  $v_Q$  in the excluded space. These are found to have the following form:

$$(N(\lambda \mu) \ KJ \mid v_{O} \mid N\bar{\lambda}\bar{\mu}\bar{K}J) = x\hbar\omega_{0} \sum W(JJ''\bar{J}'2; J'\bar{J}'')\{(\delta_{N1}\Delta + \delta_{N2}) \\ \times ((80) \ 0J'(20) \ J'' \mid (\lambda \mu) \ KJ)((80) \ 0\bar{J}'(20) \ \bar{J}'' \mid (\bar{\lambda}\bar{\mu}) \ \bar{K}L) \\ \times ((80) \ 0J' \parallel Q \parallel (80) \ 0\bar{J}')((20) \ J'' \parallel Q \parallel (20) \ \bar{J}'') \\ + \delta_{N3}((60) \ 0J'(40) \ J'' \mid (\lambda \mu) \ KJ)((60) \ 0\bar{J}'(40) \ \bar{J}'' \mid (\bar{\lambda}\bar{\mu}) \ \bar{K}J) \\ \times ((60) \ 0J \parallel Q \parallel (60) \ 0\bar{J}')((40) \ J'' \parallel Q \parallel (40) \ \bar{J}'')\}$$
(3.9)

where  $\Delta=1$  unless  $(\lambda\mu)$  or  $(\bar{\lambda}\bar{\mu})=(10,0)$  in which case  $\Delta=0$ . The sum  $\Sigma$  is over  $J',\,J'',\,\bar{J}',\,$  and  $\bar{J}''$ . The separable nature for this matrix element in Eq. (3.9) arises from the special exchange character of the interaction  $v_Q$ .

As is clear from Eq. (3.9), the interaction matrix in the excluded space is non-diagonal in the  $|N(\lambda L)KJ\rangle$  representation. It is convenient to transform to the diagonal representation which we denote by  $|\alpha J\rangle$ 

$$|\alpha J\rangle = \sum_{N\lambda\mu K} \langle N(\lambda\mu) KJ | \alpha J\rangle | N(\lambda\mu) KJ\rangle.$$
 (3.10)

The transformation matrix  $\langle N(\lambda L) KJ \mid \alpha J \rangle$  is given by the normalized eigenvectors in the diagonalization of the interaction matrix in the excluded space. The diagonal

elements  $\langle \alpha J \mid H_A \mid \alpha J \rangle = \xi_{\alpha J}$  are the eigenvalues. In terms of the diagonal representation, the bb-vertex renormalization (to all orders) of the first-order wave operator in Eq. (3.4) takes the form

$$\langle \alpha J \mid \vec{W}_{bb} \mid 80 \ 0J \rangle = \frac{1}{(1 - \vec{\xi}_{\alpha J})} (\alpha J \mid v_Q \mid 80 \ 0J) / (-2\hbar\omega_0)$$
 (3.11a)

where

$$\bar{\xi}_{\alpha J} = \xi_{\alpha J}/(-2\hbar\omega_0)$$

OF

$$\langle N(\lambda \mu) \ KJ \mid \vec{W}_{bb} \mid 80 \ 0J \rangle = \sum_{N'\lambda'\mu'K'J'} \langle N\lambda \mu KJ \mid \alpha J \rangle \frac{1}{(1 - \bar{\xi}_{\alpha J})} \langle \alpha J \mid N'\lambda \ \mu'K'J \rangle \times \langle N'\lambda'\mu'K'J \mid v_O \mid 80 \ 0J \rangle / (-2\hbar\omega_0). \tag{3.11b}$$

In Eq. (3.9) we note that the interaction matrix elements within the excluded spaces N=1 or 2 have, as factors, the reduced quadrupole matrix elements within the (80)-model space. Again, according to the principle of consistent renormalization, these factors should be replaced by the renormalized value as in Eq. (3.8) when allowing also for bd-renormalization. For the N=3 space ( $sd \rightarrow sdg$  excitation) the transformation within the model space is given by the quadrupole matrix elements within the ( $\lambda\mu$ ) = (60) representation corresponding to the structure of the three remaining sd-particles after the excitation of the fourth to the sdg-shell. We have approximated the bd-renormalization of this term by assuming the  $\epsilon_{J'J}$  for the (60)-quadrupole matrix element is the same as that in Eq. (3.8) for the (80)-matrix element. In general then the  $\overline{W}$ -function,  $\overline{W}_{bb}(\epsilon)$ , itself depends in a highly nonlinear way on the enhancement factors  $\epsilon_{JJ'}$ .

On substituting for the matrix elements of  $W^{(1)} oup W_{bb}$  ( $\epsilon = 1$ ) from Eq. (3.11) into Eqs. (3.5) and (3.6) we obtain, respectively, the enhancement factors  $\epsilon_{JJ'}$  (Fig. 3, crosses labeled c) and the energy spectrum (Fig. 2c) in the bb-approximation. If Eq. (3.5) is solved (iteratively) with  $W^{(1)} oup W_{bb}(\epsilon)$ , with  $\epsilon$  having the self-consistent value, we generate the bd-vertex renormalization upon the black box (bb-bd). The bb-bd results for  $\epsilon_{JJ'}$  and the energy spectrum are those labeled e in Figs. 3 and 2, respectively.

We note that the black-box renormalization by itself does not yield a significantly different enhancement factor or spectrum over similar quantities derived in the first-order calculation (compare the results b and c in Figs. 3 and 2). However, the bb-renormalization is enhanced by the self-consistent bd-renormalization such that the difference between the self-consistent results with and without the bb-vertex renormalization can be considerable (compare the results d and e in Figs. 2 and 3).

# The IBG Terms

In I it was noted that, for the renormalization in the intrinsic frame, a contribution in second order to the quadrupole enhancement from a diagram we called the inter-

mediate bubble generating diagram (IBG) was equal to the second-order contribution arising from the bb-renormalization of the bubble diagram. The addition of the IBG diagram takes the form

$$\sum \left[ \langle 80 \ 0J \| \widehat{W}^{(1)} \| N(\lambda \mu) \ KJ \rangle \langle N\lambda \mu KJ \| Q \| N\lambda \mu KJ' \rangle \langle N\lambda \mu KJ' \| \widehat{W}^{(1)} \| 80 \ 0J' \rangle \right. \\
\left. - \frac{1}{2} \{ \langle 80 \ 0J \| \widehat{W}^{(1)} \| N\lambda \mu KJ \rangle \langle N\lambda KJ \| \widehat{W}^{(1)} \| 80 \ 0J \rangle \right. \\
\left. + \langle 80 \ 0J' \| \widehat{W}^{(1)} \| N\lambda \mu KJ' \rangle \langle N\lambda \mu KJ' \| \widehat{W}^{(1)} \| 80 \ 0J' \rangle \} (80 \ 0J \| Q \| 80 \ 0J') \right] (3.12)$$

where the sum  $\Sigma$  is over all intermediate states  $|N(\lambda\mu)|KJ\rangle$ . For renormalization up to second order the first-order values for  $\vec{W}^{(1)}$  would be used in Eq. (3.12) but clearly by making the substitution  $\vec{W}^{(1)} \to \vec{W}_{bb}(\epsilon)$  we can generalize Eq. (3.12) to include the bb-vertex renormalization with the self-consistent bd-renormalization. The addition of Eq. (3.12) to Eq. (3.5) in the evaluation of the renormalization of quadrupole matrix elements yields the full bb-bd-IBG approximation.

Corresponding to the addition of the term in Eq. (3.12) to Eq. (3.5) for the quadrupole matrix element, we must add to Eq. (3.6), for the effective interaction, the term

$$\frac{1}{2}[(80\ 0J \mid \widetilde{W}^{(1)} \mid N\lambda\mu KJ) \langle N\lambda\mu KJ \mid v_{o} \mid N'\lambda'\mu'K'J' \rangle \langle N'\lambda'\mu'K'J' \mid \widetilde{W}^{(1)} \mid 80\ 0J) \\
- (80\ 0J \mid \widetilde{W}_{sb} \mid 80\ 0J)]$$
(3.13a)

where

$$(80 \ 0J \mid \tilde{W}_{sb} \mid 80 \ 0J) = \langle 80 \ 0J \mid v_Q \mid \alpha J \rangle \frac{\bar{\xi}_{\alpha J}}{(1 - \bar{\xi}_{\alpha J})^2} (\alpha J \mid v_Q \mid 80 \ 0J) / (-2\hbar\omega_0) \quad (3.13b)$$

with  $\bar{\xi}_{\alpha J}$  defined in Eq. (3.11). As was discussed in I the term in Eq. (3.13b) removes double counting originating from the use of the  $\epsilon_{JJ'}$  arising from the bb-bd-IBG approximation in the first terms of Eq. (3.6).

The values for the renormalized quadrupole matrix elements in the full bb-bd-IBG approximation are given in Fig. 3, crosses labeled g, and the corresponding spectrum in Fig. 4, spectrum g. In paper I we saw that the bb-bd-IBG approximation as applied in the intrinsic frame reproduced very well the properties of the deformed Hartree-Fock state. Now we see that this same approximation as applied in the laboratory frame has many of the features of the variation-after-projection Hartree-Fock approach. It is difficult to assess why the differences between the bb-bd-IBG and VPHF approximations occur since we do not have the complete analytic structure for either the renormalization approach or the VPHF approach in the laboratory frame. A possible source of error is in our estimate of the bd self-consistent renormalization in the black box for the valence polarization terms ( $sd \rightarrow sdg$ ). We recall that there we assumed the renormalization factor associated with the three remaining sd-particles was similar to that for four. It is possible (but difficult) to treat this term precisely without any assumption. We feel, however, that the closeness of the agreement of our present bb-bd-IBG results and VPHF has already demonstrated the

degree of complexity and self-consistency that must enter into the renormalization of operators within the spherical shell model in order to recapture collective effects.

#### Perturbation Order

In the first-order (bubble) correction to the quadrupole matrix elements the wave operator is taken to first order in Eq. (3.5). The bd-self-consistent renormalization of this term is found by the substitution  $\vec{W}^{(1)} \to \vec{W}(\epsilon)$  and solving for  $\epsilon_{II'}$ . It is convenient to find the solution by an iterative technique the results for which are given in Fig. 6d. These diagrams for each J-J' pair correspond to the single diagram of Fig. 4 in I for the renormalization of the intrinsic quadrupole matrix element. In Fig. 6 we plot on the ordinate the  $\epsilon_{II'}$  from the nth iteration (i.e., from the LHS of Eq. (3.5) with  $\vec{W}^{(1)} \rightarrow \vec{W}(\epsilon)$  and on the abscissa the  $\epsilon_{II'}$  from the (n-1)th iteration introduced into the RHS of Eq. (3.5). The various places in the iteration are marked by crosses. Clearly the self-consistent point is reached when the iterative curve crosses the 45° line (i.e.,  $\epsilon_{\rm in} \equiv \epsilon_{\rm out}$ ). In the  $(\vec{W}^{(1)} \to \vec{W}^{(1)}(\epsilon))$  approximation this point is reached only after about five iterations starting with  $\epsilon_{II'} = 1$ . Note that since the first iteration ( $\epsilon_{in} = 1$ ) corresponds to first-order perturbation theory, the second iteration corresponds to the addition of some second-order terms, etc. Thus selfconsistency cannot be reached before the addition of some fifth-order terms in perturbation theory at least.

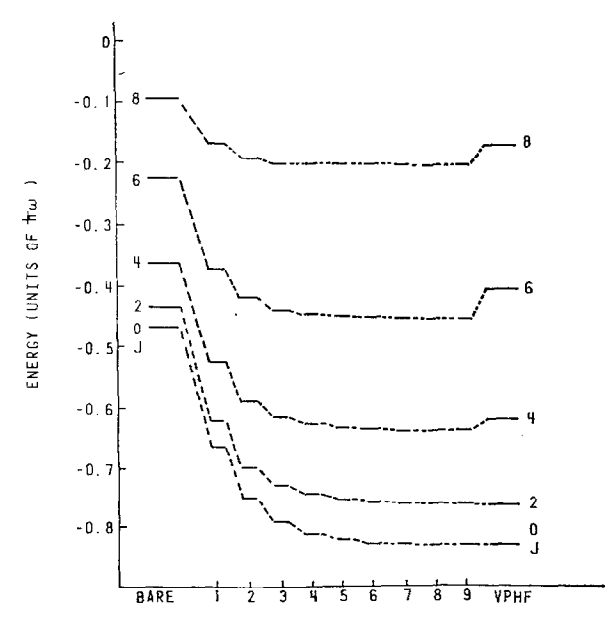


Fig. 7. Changes in the energy spectrum for <sup>20</sup>Ne throughout the iterative sequence of the bb-bd-IBG approximation for  $H_A$  (x = -0.003).

TABLE I

Values for the Enhancement Factors  $\epsilon_{IJ}$  in the Bubble, Black-Box, and IBG Approximation (c' of Fig. 5) and, in Brackets, the Black-Dot, Black-Box, and IBG Approximation (g of Fig. 5) for Various Restrictions on the Sums of Intermediate States Shown in Columns 2 and 3 and Distinguished by Roman Numerals in Column 1

	Interm	Intermediate states	Trai	nsition matri	Transition matrix elements (J-J')	f-J')	M	Moment matrix elements (J-J)	κ elements (J	(r-
	N	$(\lambda\mu)$	2-0	2-0 4-2 6-4		8-6	2-2	4	4-4 6-6	8-8
	2	(10, 0)	1.15 (1.18)	1.14 (1.17)	1.15 (1.18) 1.14 (1.17) 1.14 (1.17) 1.14 (1.16)	1.14 (1.16)	1.14 (1.17)	1.14 (1.17) 1.12 (1.14) 1.09 (1.10) 1.05 (1.05)	1.09 (1.10)	1.05 (1.05)
≔	7	(10,0) + (81)	1.17 (1.17)	1.17 (1.17)	1.17 (1.17) 1.17 (1.17) 1.16 (1.16) 1.15 (1.16)	1.15 (1.16)	1.16 (1.17)	1.16 (1.17) 1.14 (1.14) 1.10 (1.10) 1.06 (1.06)	1.10 (1.10)	1.06 (1.06)
Ξ	2	(10, 0) + (81) + (62)	1.20 (1.27)	1.20 (1.26)	1.20 (1.27) 1.20 (1.26) 1.20 (1.25) 1.19 (1.24)	1.19 (1.24)	1.20 (1.26)	1.20 (1.26) 1.19 (1.24) 1.18 (1.22) 1.17 (1.21)	1.18 (1.22)	1.17 (1.21)
iv	1 + 2	(10, 0)	1.15 (1.18)	1.14 (1.17)	1.15 (1.18) 1.14 (1.17) 1.14 (1.17) 1.14 (1.16)	1.14 (1.16)	1.14 (1.17)	1.14 (1.17) 1.12 (1.14) 1.09 (1.10) 1.05 (1.05)	1.09 (1.10)	1.05 (1.05)
>	1 + 2	(10,0) + (81).	1.14 (1.17)	1.14 (1.17)	1.14 (1.17) 1.14 (1.17) 1.14 (1.16) 1.13 (1.15)	1.13 (1.15)	1.14 (1.16)	1.14 (1.16) 1.12 (1.14) 1.09 (1.11) 1.06 (1.07)	1.09 (1.11)	1.06 (1.07)
, <b>z</b>	1 + 2	(10,0) + (81) + (62)	1.21 (1.28)	1.21 (1.28)	1.21 (1.28) 1.21 (1.28) 1.21 (1.27) 1.20 (1.26)	1.20 (1.26)	1.21 (1.28)	1.21 (1.28) 1.21 (1.27) 1.20 (1.26) 1.21 (1.26)	1.20 (1.26)	1.21 (1.26)
vii	3	(10, 0)	1.17 (1.22)	1.17 (1.22)	1.17 (1.22) 1.17 (1.22) 1.17 (1.21) 1.17 (1.20)	1.17 (1.20)	1.17 (1.21)	1.17 (1.21) 1.14 (1.18) 1.11 (1.13) 1.06 (1.07)	1.11 (1.13)	1.06 (1.07)
viii	3	(10, 0) + (81)	1.18 (1.23)	1.18 (1.22)	1.18 (1.23) 1.18 (1.22) 1.17 (1.21) 1.17 (1.20)	1.17 (1.20)	1.17 (1.21)	1.17 (1.21) 1.14 (1.18) 1.10 (1.13) 1.04 (1.06)	1.10 (1.13)	1.04 (1.06)
Χ	3	(10,0) + (81) + (62)	1.19 (1.25)	1.19 (1.24)	1.19 (1.25) 1.19 (1.24) 1.19 (1.23) 1.18 (1.22)	1.18 (1.22)	1.18 (1.23)	1.18 (1.23) 1.16 (1.20) 1.11 (1.15) 1.07 (1.09)	1.11 (1.15)	1.07 (1.09)
×	1 + 2 + 3	(10, 0)	1.32 (1.54)	1.32 (1.51)	1.32 (1.54) 1.32 (1.51) 1.31 (1.48) 1.31 (1.44)	1.31 (1.44)	1.30 (1.50)	1.30 (1.50) 1.26 (1.42) 1.19 (1.30) 1.11 (1.15)	1.19 (1.30)	1.11 (1.15)
Σ.	1 + 2 + 3	(10, 0) + (81)	1.32 (1.54)	1.32 (1.51)	1.32 (1.54) 1.32 (1.51) 1.31 (1.48) 1.30 (1.44)	1.30 (1.44)	1.30 (1.50)	1.30 (1.50) 1.26 (1.42) 1.19 (1.29) 1.11 (1.15)	1.19 (1.29)	1.11 (1.15)
xii	1 + 2 + 3	(10,0) + (81) + (62)	1.40 (1.83)	1.40 (1.77)	1.40 (1.83) 1.40 (1.77) 1.39 (1.72) 1.39 (1.67)	1.39 (1.67)	1.39 (1.76)	1.39 (1.76) 1.36 (1.66) 1.32 (1.54) 1.27 (1.41)	1.32 (1.54)	1.27 (1.41)

Shown also in Fig. 6, by the crosses on lines g, is the iterative sequence for the full bb-bd-IBG approximation. With just the bb-renormalization (no bd-iteration) the enhancement value for the J-J'=2-0 matrix element is 1.4 (compared to the first-order bubble value of 1.35). After reaching self-consistency the bb-bd-IBG value for  $\epsilon_{20}$  is  $\sim$ 1.88 (compared to)the value of 1.54 for the iterative bubble approximation). Clearly the higher-order terms in the bb-renormalization are very important in the iterative (self-consistent) process to achieve the large collective enhancement factors. Again one needs to iterate at least five times to get near self-consistency. We note that the second-order term in the black box effectively yields perturbation terms of the 10th order at the 5th iteration. Thus the full self-consistent bb-bd-IBG approximation involves certain classes of diagrams to very high perturbative order. To try to include such diagrams explicitly by a straightforward summation technique is clearly impractical: some technique like infinite summation (as in the bb-series) or iteration (as in the bd-renormalization) must be used to capture the main effect of these higher order terms without explicitly having to write them down.

In Fig. 7 we show the changes in the spectrum during the iterative procedure leading up to the full bb-bd-IBG approximation. This figure shows that the iterative technique is simulating the change of spectrum from the far LHS of Fig. 1 to the position of the minima. Clearly the energies (and enhancement factors) associated with the low J states are the slowest to converge taking at least five iterations.

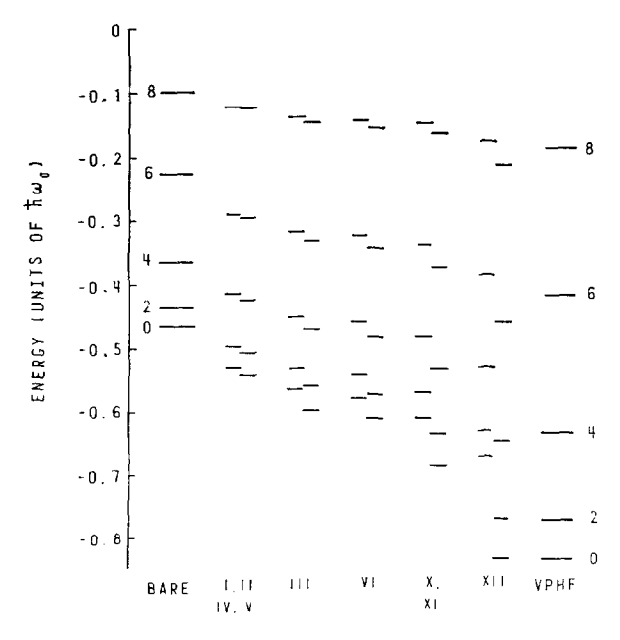


Fig. 8. Energy spectra corresponding to the various "excluded" states considered in the perturbation series as listed in Table I, and defined by the Roman numerals. Similar spectra have only been drawn once, but given multiple labels.

#### Core and Valence Polarization

Summations in the perturbation series over excluded states having N=1  $(1s \rightarrow (2s, 1d))$  excitations) and N=2  $(1p \rightarrow (2p, 1f))$  excitations) contribute to the so-called core polarization: the terms having N=3  $((2s, 1d) \rightarrow (3s, 2d, 1g))$  yield the polarization of the valence orbits. In each of these categories there are contributions from states having  $(\lambda \mu) = (10, 0)$ , (81), and (62)  $SU_3$  symmetry. In Table I we show the results for the enhancement values of the bb-bubble-IBG approximation (and, in brackets, the full bb-bd-IBG approximation) but with various limitations on the intermediate states considered. Some of the corresponding spectra have been drawn in Fig. 8. We conclude from these results that valence polarization is as important as core polarization for this schematic Hamiltonian at least (a feature in common with the intrinsic calculation of 1) and the most important states in these categories have the  $(\lambda \mu) = (10, 0)$  and (6, 2)  $SU_3$  symmetry.

# 4. SUMMARY AND GENERALIZATIONS

Our aim in this paper has been to compare the numerical results for quadrupole matrix elements and spectra in the projected Hartree-Fock approaches and the renormalized spherical shell model for the schematic quadrupole-quadrupole Hamiltonian  $H_A$ . We have demonstrated that similar results can be obtained for the VPHF model and the renormalized shell model with wave operator calculated in the bb-bd-IBG approximation. Our analysis suggests that some very high order (>10) perturbation terms must be included if the collective features of the Hartree-Fock model are to be adequately recaptured in the renormalized spherical shell model.

In a paper by Harvey and Khanna [14] the sentiment was expressed that if one is forced into a phenomenological treatment of the spherical shell model, because the orders of perturbation are too large for an adequate renormalization, then the object that should be parameterized is the wave operator  $\vec{W}$  (referred to as the "coupling-operator" in [14]). One approach to determine the appropriate structure for  $\vec{W}$  is to first understand what physical features are not adequately described by the bare model and then ask how these features must manifest themselves in  $\vec{W}$ . In I and this paper we have attempted to construct a  $\vec{W}$  that recaptures the collective (deformation) characteristics of the unrestricted deformed Hartree-Fock model. Since the single particle field in the Hartree-Fock model arises from a self-consistent procedure, it is natural that  $\vec{W}$  should itself be determined through an iterative scheme.

In seeking the equivalence within the spherical shell model of deformed Hartree–Fock for a realistic interaction we clearly would like to develop a technique by which higher-order perturbation terms associated with the "collective renormalization" (equivalence of bb-bd-IBG) can be summed by the iteration method so that we stay close to the self-consistency aspects of the structure. We also desire the technique to be tractable for any number of valence nucleons. The problem with generalizing the results in I and this paper is that a realistic ineraction does not have a separable form

and hence no natural multipole operator (like Q) with which to use the black-dot consistent-renormalization simplification. It must also be realized that the valence polarization is relatively more important than the core polarization the more particles there are in the valence shell. Thus one must treat with greater care the excitations from and into these partially filled orbitals. Already we have seen in this paper that the approximations we used to handle the valence polarization may not be adequate.

The most promising approach to "collective renormalization" being pursued at this time by one of us (M.H.) in collaboration with I.S. Towner is to consider directly the evaluation of the transition-density matrices

$$\rho_{yx}(AB) = \langle A \mid \eta_x^{\dagger} \eta_y \mid B \rangle \tag{4.1}$$

where  $\eta_y^{\dagger}(\eta_y)$  creates (destroys) a particle in the single particle orbital y. Here A and B denote any two states of the many particle nucleus. Clearly for any single particle operator like Q

$$\langle A \mid Q \mid B \rangle = \sum_{xy} Q_{xy} \rho_{yx} (AB).$$
 (4.2)

If the states A and B are approximated in zeroth order by spherical shell model states, then the only nonzero transition-density matrix elements are those for which x and y are both the same core (c) orbital or both some valence (v) orbitals. In this case the  $\rho_{yx}(AB)$  are given by products of coefficients of fractional parentage (cfp). Other components of the transition-density matrices arise from the perturbation series. Thus, for example if x is a core (c) orbital and y an excluded (e) orbital, in first-order perturbation theory,

$$\rho_{ec}^{(1)}(AB) = G_{eacb}\rho_{ba}(AB)/E_{ec}$$

where a and b are core or valence orbitals. Here G represents a realistic two-body interaction appropriate for independent (quasi)-particle motion and  $E_{ee}$  is the energy difference between the core and excluded orbitals. The second-order contribution to  $\rho_{ee}(AB)$  from the Tamm-Dancoff series has the structure

$$\rho_{ec}^{(2)}(AB) = G_{ee'cc'}G_{e'ac'b}\rho_{ba}(AB)/E_{ec}E_{e'c'}$$

$$\equiv G_{ec'cc'}\rho_{c'c'}^{(1)}(AB)/E_{ec}.$$
(4.3)

The full Tamm-Dancoff approximation for  $\rho_{ec}(AB)$  is thus given by

$$E_{ec}\rho_{ec}(AB) = G_{eacb}\rho_{ba}(AB) + G_{ee'cc'}\rho_{e'c'}(AB). \tag{4.4}$$

This set of equations (all e, c) can be solved exactly for the  $\rho_{ec}(AB)$  but, for later considerations, is best considered solved by iteration starting with the value zero for all  $\rho_{e'e'}(AB)$  on the RHS of Eq. (4.4). The RPA approximation is obtained by adding to the RHS of Eq. (4.4) the term

$$G_{\alpha\alpha'\alpha\alpha'}\rho_{\alpha'\alpha'}(AB) \tag{4.5}$$

and solving simultaneously the modified set of Eqs. (4.4) with a similar set for  $\rho_{ce}(AB)$ .

Additional terms can be added to Eq. (4.4) which introduce the black-box vertex renormalization as well as valence polarization terms, etc. Each term can be written in general in terms of products of transition-density matrix elements and thus, at each iteration, contribute varying amounts to the final structure for each matrix element of  $\rho(A, B)$ .

The significance of the present approach is that by considering the renormalization of the single particle transition densities we stay close to the Hartree-Fock technique although now we do not restrict the states A, B to be a single determinant but rather allow them to develop, by the (iterative) perturbation series (like Eq. (4.4)), from the spherical shell model states. For a given nucleus the only input are the transition density matrix elements in the model space  $\rho_{ab}(AB)$  determined from the cfp's. Thus in principle the technique is applicable wherever cfp's are available independent of the number of valence particles. In practice the calculation does become more complicated the more particles are added into the valence shell. These complications together with preliminary results must await a further publication.

To see that the renormalization of the density is equivalent to the bb-bd-IBG approximation in I consider in the generalized form for Eq. (4.4) the states A and B to be the intrinsic state  $\chi_{\delta}$  with normalized component  $\chi_{0}$  in the model space. Consider also G to be separable, i.e.,  $G_{abcd} \equiv Q_{ac}Q_{db}$ . Now the generalized Eq. (4.4) will take the form

$$E_{ec}\rho_{ec}(\chi_{\delta},\chi_{\delta}) = Q_{ec}(Q_{ab}\rho_{ba}(\chi_{0}\chi_{0}) + Q_{c'e'}\rho_{e'c'}(\chi_{\delta}\chi_{\delta}) + ...)$$

$$\equiv Q_{ec}\langle\chi_{\delta} \mid Q \mid \chi_{\delta}\rangle. \tag{4.6}$$

Thus from Eq. (4.2), the expectation value of Q in the fully renormalized (deformed) intrinsic state  $\chi_{\delta}$  has the form

$$\langle \chi_{\delta} | Q | \chi_{\delta} \rangle \equiv \langle Q \rangle_{\delta} = Q_{ab} \rho_{ba} (\chi_{0} \chi_{0}) + Q_{ce} \rho_{ec} (\chi_{\delta} \chi_{\delta}) + Q_{ec} \rho_{ce} (\chi_{\delta} \chi_{\delta}) + \cdots$$

$$\equiv \langle Q \rangle_{0} + 2 \frac{Q_{ce} Q_{ec}}{E_{ec}} \langle Q \rangle_{\delta} + \cdots, \tag{4.7}$$

the last line coming from the substitution from Eq. (4.6). It was just this latter equation which was shown in I to be equivalent to the self-consistent Hartree-Fock condition given in this paper by Eq. (1.6).

# ACKNOWLEDGMENT

One of us (P.A.) wishes to thank G. A. Bartholomew for the hospitality in the Physics Division, Chalk River during the Summer 1974.

#### REFERENCES

- E. C. HALBERT, J. B. McGRORY, B. H. WILDENTHAL, AND S. P. PANDYA, in "Advances in Nuclear Physics" (M. Baranger and E. W. Vogt, Ed.) Vol. 4, p. 316, Plenum, New York/London, 1971.
- 2. B. R. BARRETT AND M. KIRSON, in "Advances in Nuclear Physics" (M. Baranger and E. W. Vogt, Eds.), Vol. 6, p. 219, Plenum, New York/London, 1973.
- 3. R. Y. Cusson and H. C. Lee, Nucl. Phys. A 211 (1973), 429.
- 4. M. HARVEY, Ann. Phys. (N.Y.) 94 (1975), 47.
- 5. M. Harvey, in "Advances in Nuclear Physics" (M. Baranger and E. W. Vogt, Eds.), Vol. 1, p. 67, Plenum, New York/London, 1968.
- 6. B. R. MOTTELSON, L'École d'Été de Physique Théorique, Les Houches, Paris, 1959.
- G. RIPKA, in "Advances in Nuclear Physics" (M. Baranger and E. W. Vogt, Eds.), Vol. 1, p. 183, Plenum, New York/London, 1968.
- 8. G. SAUNIER AND J. M. PEARSON, Phys. Rev. C 1 (1970), 1353.
- 9. J. P. ELLIOTT AND M. HARVEY, Proc. Roy. Soc. Ser. A 272 (1963), 557.
- M. Harvey, "Proc. Int. School of Physics "Enrico Fermi" Course LXII, Varenna" (H. Faraggi and R. A. Ricci, Eds., 1974, North Holland, Amsterdam/New York/Oxford, 1976.
- 11. K. T. HECHT, Nucl. Phys. 62 (1965), 1.
- 12. T. Sebe, Nucl. Phys. A 109 (1968), 65.
- 13. M. ROTENBERG, R. BIVIMS, N. METROPOLIS, AND K. K. WOOTEN, JR., "The 3-j and 6-j Symbols," The Technology Press, Massachusetts Institute of Technology, Cambridge, 1959.
- 14. M. HARVEY AND F. C. KHANNA, Nucl. Phys. A 155 (1970), 337.